

## Prediction and assessment of nonlocal natural frequencies of DWCNTs: Vibration analysis

Sehar Asghar<sup>1a</sup>, Muhammad N. Naeem<sup>1</sup>, Muzamal Hussain<sup>\*1</sup>, Muhammad Taj<sup>2</sup> and Abdelouahed Tounsi<sup>3,4</sup>

<sup>1</sup>Department of Mathematics, Govt. College University Faisalabad, 38040, Faisalabad, Pakistan

<sup>2</sup>Department of Mathematics, University of Azad Jammu and Kashmir, Muzaffarabad, 1300, Azad Kashmir, Pakistan

<sup>3</sup>Materials and Hydrology Laboratory, University of SidiBel Abbes, Algeria Faculty of Technology Civil Engineering Department, Algeria

<sup>4</sup>Department of Civil and Environmental Engineering, King Fahd University of Petroleum & Minerals, 31261 Dhahran, Eastern Province, Saudi Arabia

(Received December 17, 2019, Revised January 24, 2020, Accepted January 30, 2020)

**Abstract.** This paper aims to study vibration characteristics of chiral and zigzag double-walled carbon nanotubes entrenched on Donnell shell model. The Eringen's nonlocal elastic equations are being combined with Donnell shell theory to observe small scale response. Wave propagation is proposed technique to establish field equations of model subjected to four distinct end supports. A nonlocal model has been formulated to explore the frequency spectrum of both chiral and zigzag double-walled CNTs along with diversity of indices and nonlocal parameter. The significance of scale effect in relevance of length-to-diameter and thickness- to- radius ratios are discussed and displayed in detail. The numerical solution based on this nonlocal Donnell shell model can be further used to predict other frequency phenomena of double-walled and multi-walled CNTs.

**Keywords:** CNT; Chiral and zigzag; nonlocal parameter; Donnell shell model

### 1. Introduction

Since from the last decade carbon nanotubes (CNTs) have become potential subject of scientific research with its vigorous performance in the various fields. Owing to remarkable physical and mechanical features of the nano-sized structures, they have been persuasive and contemporary measure in aerospace, microscopic system, actuators, gas exposure, defence, diagnosis devices and several more. (Lau and Hui 2002, Zhao 2002, Lieber 2003, Liu and Zang 2004, Kostarelos *et al.* 2009, Sosa *et al.* 2014, Fakhrabadi *et al.* 2015). CNTs also contribute significantly in material science, medicine and structural engineering (Gittes *et al.* 1993, Nogales 2001, Kasas *et al.* 2004, Regi 2007, Reilly 2007, Gohardani *et al.* 2014, Soldano 2015). Basically CNTs are in shape of cylindrical macromolecules composed of carbon atoms attracted astounding response from scientific community. Over the last number of years, CNTs have become focus of interest amidst leading scientists from many research areas. CNTs are exceptionally meagre in structure, so to envision the behaviour through experimental techniques of such nanostructures under various conditions is not an easy task.

For that reason, computational simulations have been taken an edge being dynamic tool to inspect the physical and mechanical attributes of CNTs. The past research work found on nanotubes carried out by two main methodologies

known as continuum mechanics and molecular dynamics (MD). The MD simulation approach is a presentation of molecules of the materials which is distinct solution of Newton's classical equations of motion and has been efficiently exercised to analyse the dynamical properties of single-, double- and multi-walled CNTs (Cornwell and Wille 1997, Liew *et al.* 2005, Hao *et al.* 2008, Hu *et al.* 2008). At the same time, continuum mechanics has been engaged to examine various features of minuscule and nano-sized suchlike thermo mechanical investigations (Murmur and Adhikari 2010, Rafiee and Moghandam 2014), buckling (Chang *et al.* 2005, Wang *et al.* 2006, Lu *et al.* 2007) and free vibrations (Xu *et al.* 2008, Hu *et al.* 2012, Chang and Lee 2009, Avcar 2019) of CNTs. In recent times, some of the researchers made use of continuum shell model to inquire further advancements in CNTs (Li and Kardomateas 2007, Hu *et al.* 2012, Brischetto 2014). The theory of non-local elasticity happened to be intrinsic factor in continuum mechanics by accommodating the size dependency in nanostructures introduced by Eringen (1983, 2002). The use of nonlocal continuum mechanics evolved scale effect which conferred the vibrational analysis of CNTs (Eringen 1972, Zang *et al.* 2005, Heireche *et al.* 2008, Ansari *et al.* 2012, Zidour *et al.* 2014, Benguediab *et al.* 2014). The nonlocal elasticity theory has been extensively utilized for different types of nanostructures such as nano FGM structures (Jung and Han 2013, Kolahchi *et al.* 2015, Nejad *et al.* 2016) and static (Wang and Liew 2007, Pradhan and Reddy 2011, Eltahir *et al.* 2013). The double-walled CNTs are coaxial nano structure in nature comprised of certainly two single-walled CNTs encapsulated one in other. Mehar *et al.* (2016) modeled mathematically based on the higher order shell theory. The material properties of

\*Corresponding author, Ph.D.

E-mail: muzamal45@gmail.com

<sup>a</sup>Ph.D Scholar

carbon nanotube reinforced composite plate are assumed to be temperature dependent and graded in the thickness direction using different grading rules. The structure of double-walled CNT makes it rudimentary course of action to estimate the aftermath of inter wall coupling hinge on the assorted substantial properties of CNTs. On comparing the single-walled to double-walled CNTs, it is observed that double-walled CNTs demonstrate strong mechanical ability, thermal combat and effective electronic characteristics. Free vibration of double-walled CNTs (Xu *et al.* 2008) showed explicitly the interaction of van der Waals forces being two exclusive beams. The small-scale diameters/aspect ratios were main focus for investigation which revealed the valid use of Donnell shell theory for vibration study (Hashemi *et al.* 2012). Moreover, a precise study was carried out on resonant frequencies of double-walled CNTs subjected to layer wise end conditions (Rouhi *et al.* 2013). The technique employed to obtain the numerical outcomes for ruling equations was radial point interpolation differential quadrature (RPIDQ) based on nonlocal Donnell shell theory which happened to justify the scale effects. Mehar and Panda (2018) investigated the curved shell and CNT vibration with thermal environment using higher order deformation theory. These CNT was mixed with different configurations of the layers. The results have been verified with the earlier investigations.

Among armchair, chiral and zigzag single and double-walled CNTs, limited work is done related to chiral and zigzag especially double-walled CNTs. The stress aspects of single-walled CNTs with respect to chiral dependency of the axial tensile strain was examined (Yoshikazm *et al.* 2005). They applied numerical simulation that worked with a tight binding and first principles density functional theory calculation depicting its authentication. Mehar and Panda (2018) computed the vibration behavior, bending and dynamic response of FG reinforced CNT finite element method. For the sake of generality, the mathematical model was presented with the mixture of Green Lagrange method. The convergence of these methodologies have been checked for the variety of results. The composite paltes with differencet greded was investigated with isotropic and core phase. (Ghavanloo and Fazlzadeh 2009) studied the vibration frequency spectra of chiral CNTs, Flugge shell theory was applied to obtain the isotropic elastic model. Timoshenko beam model framed on nonlocal elasticity theory was utilized (Zidour *et al.* 2014), they performed a study on elastic bending of chiral single-walled CNTs considering axial compression. Their work comprehensively covered the chirality of single-walled CNTs, its vibrational mode and aspect ratio against the critical buckling load. Mehar *et al.* (2017a, b) studied the freqncy response of FG CNT and reinforced CNT using the simple deformation theory and Mori-Tanaka scheme. They investigated a new frequency phenomena with the combination of Lagrange strain, Green-Lagrange, for double curved and curved panel of FG and reinforced FG CNT. The charactriotics of sandwich and grades CNT Bwas found with labeling the temperarure environ. The thermoelastic frequency of single shaollow panel was determined using Mori-Tanake formaulation. The research

of these authore have opened a new frequency spectra for other material researchers. Benguediab *et al.* (2014) inspected mechanical buckling characteristics of a zigzag double-walled CNTs incorporated with chirality and small scale effect. Their findings revealed influential reliance of critical buckling load of zigzag CNTs by using nonlocal Timoshenko beam model. Mehar *et al.* (2018) evaluated the frequency behavior of nanolpate structure using FEM including the nonlocal theory of elasticity. Computer generated results are created by using the software first time roubustly to check the vibration of nanoplate. The efficiency was checked by comparing the results of available data.

Hussain and Naeem (2017) examined the frequencies of armchair tubes using proposed approach based on Flügge's shell model. The effect of length and thickness-to-radius ratios against fundamental natural frequency with different indices of armchair tube. The increment and decrement of frequency observed on increasing the thickness-to-radius ratio and length. Chemi *et al.* (2015) exhibited frequency vibrations of chiral double-walled CNTs. The set of governing equations were modelled by nonlocal Euler Bernoulli beam theory. Batou *et al.* (2019) investigated the wave propagations in sigmoid functionally graded (S-FG) plates using Higher Shear Deformation Theory (HSDT). Salah *et al.* (2019) interpreted the ceramic-metal FGM sandwich plates using 2D integral plate model. The results were verified with the earlier investigations. Recently Hussain and Naeem (2019a, b, c, d) performed the vibration of SWCNTs based on wave propagation approach and Galerkin's method. Jamali *et al.* (2019) and Ebrahimi *et al.* (2019) studied the effects of postbukling behavior and magneto-electro-elastic curved nanotubes using different methodologies. This research opened a new window for the material researchers. Bisen *et al.* (2018) and Mehar and Panda (2019) studied the structural response of reinforced material and FG-CNT using the numerical and experimental properties. The results are verified with the open existing literature. The computer software MATLAB was used for the frequency results. The higher order finite element and higher order mid-plane kinematics. The mixture rule was defined for the different materials.

The foremost intension of this paper to investigate nonlocal vibration characteristics of zigzag and chiral double-walled CNTs by means of Donnell shell theory along with wave propagation technique, which is our intrinsic interest. The suggested method to investigate the solution of fundamental eigen relations is a well-known and efficient technique. It is carefully observed from the literature, no information is seen regarding present established model where aforementioned problem has been considered so it became an incentive to proceed current study. The specific influence of four distinct end supports based on proposed method such as clamped-clamped, clamped-simply supported, simply supported-simply supported and clamped-free is examined in detail.

Many material researchers calculated the frequency of CNTs using different techniques, for example, Timoshenko beam model (Zidour *et al.* 2014), Euler Bernoulli beam theory (Chemi *et al.* 2015), Flugge shell theory (Zidour *et*

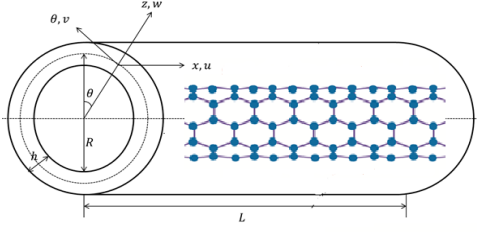


Fig. 1 Geometry of double-walled carbon nanotubes

al. 2014), nonlocal Donnell shell theory (Rouhi *et al.* 2013), and interpolation differential quadrature (Rouhi *et al.* 2013). The aim of current study is to delve for the free vibration characteristics of chiral and zigzag double-walled CNTs by forming a nonlocal Donnell shell model (DSM). Eringen's nonlocal elasticity equations are acquired by adopting DSM to count scale effect. The investigation is realized by employing the wave propagation approach due to its effective application in studying the structural vibrational analysis related to different parameters and end supports. The domination of numerous end supports alike DSM simply supported (DSM-SS), DSM clamped-supported (DSM-CS), DSM clamped-clamped (DSM-CC) and DSM clamped free (DSM-CF) regarding disparate values of nonlocal parameter are explored numerically and reflected with help of graphs.

## 2. Formulation of governing nonlocal shell equations

The theory of non-local elasticity despite of traditional elasticity, states the stress at a certain point rely upon the strain in a domain nearby that specific point. The nonlocal equation (Eringen 1983, 2002) is expressed by

$$(1 - (e_0 a)^2 \nabla^2) \sigma = t \quad (1)$$

The term  $e_0 a$  describes the characteristic length known as nonlocal parameter. The generalized Hooke's law relates stress tensor to strain as

$$t = S : \epsilon \quad (2)$$

where  $S$  stands as fourth order elasticity tensor and  $:$  indicates the double dot product. The stress and strain relationship is presented by Hooke's law as

$$\begin{Bmatrix} \sigma_{xx} \\ \sigma_{\theta\theta} \\ \sigma_{x\theta} \\ \sigma_{\theta z} \\ \sigma_{xz} \end{Bmatrix} - (e_0 a)^2 \nabla^2 \begin{Bmatrix} \sigma_{xx} \\ \sigma_{\theta\theta} \\ \sigma_{x\theta} \\ \sigma_{\theta z} \\ \sigma_{xz} \end{Bmatrix} = \begin{pmatrix} E & \nu E & 0 & 0 & 0 \\ 1-\nu^2 & 1-\nu^2 & 0 & 0 & 0 \\ \nu E & E & 0 & 0 & 0 \\ 1-\nu^2 & 1-\nu^2 & 0 & 0 & 0 \\ 0 & 0 & G & 0 & 0 \\ 0 & 0 & 0 & G & 0 \\ 0 & 0 & 0 & 0 & G \end{pmatrix} \begin{Bmatrix} \epsilon_{ox} \\ \epsilon_{o\theta} \\ \gamma_{ox\theta} \\ \gamma_{o\theta z} \\ \gamma_{0xz} \end{Bmatrix} \quad (3)$$

here described terms are  $E$  as Young's modulus,  $G$  as shearing modulus and  $\nu$  as Poisson's ratio respectively. The cylindrical shell is considered the length  $L$ , thickness  $h$  and the radius  $R$  for individual tube of double-walled CNTs having coordinate system  $(x, \theta, z)$  as labelled in Fig. 1. The displacement components are described by  $u_x, u_y, u_z$  in three directions  $x, \theta$  and  $z$  whereas surface rotations by  $\psi_x$  and  $\psi_\theta$

according to classical shell theory.

$$\begin{aligned} u_x(x, \theta, z, t) &= u(x, \theta, t) + z\psi_x(x, \theta, t) \\ u_y(x, \theta, z, t) &= v(x, \theta, t) + z\psi_\theta(x, \theta, t) \\ u_z(x, \theta, z, t) &= w(x, \theta, t) \end{aligned} \quad (4)$$

The expressions that shows the accordance between normal and shear strains are written as

$$\begin{aligned} \epsilon_{ox} &= \frac{\partial u}{\partial x}, \epsilon_{o\theta} = \frac{1}{R} \frac{\partial v}{\partial \theta} + \frac{w}{R}, \gamma_{ox\theta} = \frac{1}{R} \frac{\partial u}{\partial \theta} + \frac{\partial v}{\partial x} \\ \gamma_{oxz} &= \frac{\partial w}{\partial x} + \psi_x, \gamma_{o\theta z} = \frac{1}{R} \frac{\partial w}{\partial \theta} + \frac{v}{R} + \psi_\theta \end{aligned} \quad (5)$$

Utilizing Eqs. (3)-(5) nonlocal force and moment resultants takes the form

$$N_{xx} = \int_{-h/2}^{h/2} \sigma_{xx} dz \quad \text{i.e. } N_{xx} - (e_0 a)^2 \nabla^2 N_{xx} = \frac{Eh}{1-\nu^2} \frac{\partial u}{\partial x} + \frac{\nu Eh}{1-\nu^2} \left( \frac{1}{R} \frac{\partial v}{\partial \theta} + \frac{w}{R} \right) \quad (6a)$$

$$N_{\theta\theta} = \int_{-h/2}^{h/2} \sigma_{\theta\theta} dz \quad \text{i.e. } N_{\theta\theta} - (e_0 a)^2 \nabla^2 N_{\theta\theta} = \frac{\nu Eh}{1-\nu^2} \frac{\partial u}{\partial x} + \frac{Eh}{1-\nu^2} \left( \frac{1}{R} \frac{\partial v}{\partial \theta} + \frac{w}{R} \right) \quad (6b)$$

$$N_{x\theta} = \int_{-h/2}^{h/2} \sigma_{x\theta} dz \quad \text{i.e. } N_{x\theta} - (e_0 a)^2 \nabla^2 N_{x\theta} = Gh \left( \frac{1}{R} \frac{\partial u}{\partial \theta} + \frac{\partial v}{\partial x} \right) \quad (6c)$$

$$M_{xx} = \int_{-h/2}^{h/2} z \sigma_{xx} dz \quad \text{i.e. } M_{xx} - (e_0 a)^2 \nabla^2 M_{xx} = D \left( \frac{\nu}{R} \frac{\partial \psi_\theta}{\partial \theta} + \frac{\partial \psi_x}{\partial x} \right) \quad (6d)$$

$$M_{\theta\theta} = \int_{-h/2}^{h/2} z \sigma_{\theta\theta} dz \quad \text{i.e. } M_{\theta\theta} - (e_0 a)^2 \nabla^2 M_{\theta\theta} = D \left( \frac{1}{R} \frac{\partial \psi_\theta}{\partial \theta} + \nu \frac{\partial \psi_x}{\partial x} \right) \quad (6e)$$

$$M_{x\theta} = \int_{-h/2}^{h/2} z \sigma_{x\theta} dz \quad \text{i.e. } M_{x\theta} - (e_0 a)^2 \nabla^2 M_{x\theta} = \frac{1}{2} D (1-\nu) \left( \frac{\partial \psi_\theta}{\partial x} + \frac{1}{R} \frac{\partial \psi_x}{\partial \theta} \right) \quad (6f)$$

$$Q_{xx} = \int_{-h/2}^{h/2} z \sigma_{xz} dz \quad \text{i.e. } Q_{xx} - (e_0 a)^2 \nabla^2 Q_{xx} = Gh \left( \psi_x + \frac{\partial w}{\partial x} \right) \quad (6g)$$

$$Q_{\theta\theta} = \int_{-h/2}^{h/2} z \sigma_{\theta z} dz \quad \text{i.e. } Q_{\theta\theta} - (e_0 a)^2 \nabla^2 Q_{\theta\theta} = Gh \left( \psi_\theta + \frac{v}{R} + \frac{1}{R} \frac{\partial w}{\partial x} \right) \quad (6h)$$

$D = \frac{Eh^3}{12(1-\nu^2)}$  represents tube's arced rigidity. The

controlling equations of Donnell shell theory are given as

$$\frac{\partial N_{xx}}{\partial x} + \frac{1}{R} \frac{\partial N_{x\theta}}{\partial \theta} = I_1 \frac{\partial^2 u}{\partial t^2} + I_2 \frac{\partial^2 \psi_x}{\partial t^2} \quad (7a)$$

$$\frac{\partial N_{x\theta}}{\partial x} + \frac{1}{R} \frac{\partial N_{\theta\theta}}{\partial \theta} + \frac{Q_{\theta\theta}}{R} = I_1 \frac{\partial^2 v}{\partial t^2} + I_2 \frac{\partial^2 \psi_\theta}{\partial t^2} \quad (7b)$$

$$\frac{\partial Q_{xx}}{\partial x} + \frac{1}{R} \frac{\partial Q_{\theta\theta}}{\partial \theta} + \frac{N_{\theta\theta}}{R} + p = I_1 \frac{\partial^2 w}{\partial t^2} \quad (7c)$$

$$\frac{\partial M_{xx}}{\partial x} + \frac{1}{R} \frac{\partial M_{x\theta}}{\partial \theta} - Q_{xx} = I_2 \frac{\partial^2 u}{\partial t^2} + I_3 \frac{\partial^2 \psi_x}{\partial t^2} \quad (7d)$$

$$\frac{\partial M_{x\theta}}{\partial x} + \frac{1}{R} \frac{\partial M_{\theta\theta}}{\partial \theta} - Q_{\theta\theta} = I_2 \frac{\partial^2 v}{\partial t^2} + I_3 \frac{\partial^2 \psi_\theta}{\partial t^2} \quad (7e)$$

$I_1, I_2, I_3$  are known as inertia terms and the pressure  $p$  applied on the double-walled nanotubes through van der Waals (vdW) interaction forces.

$$p = w_i \sum_{j=1}^2 c_{ij} - \sum_{j=1}^2 c_{ij} w_j \quad (i=1,2) \quad (8)$$

$c_{ij}$  is *vdW* coefficient, depicting the pressure increment contributing from  $i$ th to  $j$ th tube.

$$c_{ij} = \left[ \frac{1001\pi\epsilon\sigma^{12}}{3a^4} E_{ij}^{13} - \frac{1120\pi\epsilon\sigma^6}{9a^4} E_{ij}^7 \right] R_j \quad (9)$$

Here C-C bond length is given by  $a = 1.42\text{\AA}$ , depth of potential by  $\epsilon$ ,  $\sigma$  as parameter concluded by equilibrium distance,  $R_j$  as radius of  $j$ th tube and  $E_{ij}^m$  be as elliptic integral which is given as

$$E_{ij}^m = (R_j + R_i)^{-m} \int_0^{\pi/2} \frac{d\theta}{(1 - K_{ij} \cos^2 \theta)^{m/2}} \quad (10)$$

being  $m$  as integer and coefficient  $K_{ij}$  is defined by

$$K_{ij} = \frac{4R_j R_i}{(R_j + R_i)^2} \quad (11)$$

While studying the double-walled CNTs, each tube can be treated as an individual shell whose vibration response can be examined by the controlling Eqs. (7a)-(7e). Thus by incorporating Eqs. (6a)-(6h) into Eqs. (7a)-(7e), the field equations take following form

$$k_{11}^{(i)} u^{(i)} + k_{12}^{(i)} v^{(i)} + k_{13}^{(i)} w^{(i)} + k_{14}^{(i)} \psi_x^{(i)} + k_{15}^{(i)} \psi_\theta^{(i)} = I_1 \ddot{u}^{(i)} + I_2 \ddot{\psi}_x^{(i)} - (e_o a)^2 \left[ I_1 \left( \ddot{u}_{xx}^{(i)} + \frac{1}{R_i^2} \ddot{u}_{\theta\theta}^{(i)} \right) + I_2 \left( \ddot{\psi}_{xx}^{(i)} + \frac{1}{R_i^2} \ddot{\psi}_{\theta\theta}^{(i)} \right) \right] \quad (12a)$$

$$k_{21}^{(i)} u^{(i)} + k_{22}^{(i)} v^{(i)} + k_{23}^{(i)} w^{(i)} + k_{24}^{(i)} \psi_x^{(i)} + k_{25}^{(i)} \psi_\theta^{(i)} = I_1 \ddot{v}^{(i)} + I_2 \ddot{\psi}_\theta^{(i)} - (e_o a)^2 \left[ I_1 \left( \ddot{v}_{xx}^{(i)} + \frac{1}{R_i^2} \ddot{v}_{\theta\theta}^{(i)} \right) + I_2 \left( \ddot{\psi}_{\theta xx}^{(i)} + \frac{1}{R_i^2} \ddot{\psi}_{\theta\theta}^{(i)} \right) \right] \quad (12b)$$

$$k_{31}^{(i)} u^{(i)} + k_{32}^{(i)} v^{(i)} + k_{33}^{(i)} w^{(i)} + k_{34}^{(i)} \psi_x^{(i)} + k_{35}^{(i)} \psi_\theta^{(i)} + w^{(i)} \sum_{j=1}^M c_{ij} - \sum_{j=1}^M c_{ij} w^{(j)} = I_1 \ddot{w}^{(i)} - (e_o a)^2 \left[ I_1 \left( \ddot{w}_{xx}^{(i)} + \frac{1}{R_i^2} \ddot{w}_{\theta\theta}^{(i)} \right) + \left( \ddot{w}_{xx}^{(i)} + \frac{1}{R_i^2} \ddot{w}_{\theta\theta}^{(i)} \right) \sum_{j=1}^2 c_{ij} - \sum_{j=1}^2 c_{ij} \left( \ddot{w}_{xx}^{(j)} + \frac{1}{R_i^2} \ddot{w}_{\theta\theta}^{(j)} \right) \right] \quad (12c)$$

$$k_{41}^{(i)} u^{(i)} + k_{42}^{(i)} v^{(i)} + k_{43}^{(i)} w^{(i)} + k_{44}^{(i)} \psi_x^{(i)} + k_{45}^{(i)} \psi_\theta^{(i)} = I_2 \ddot{u}^{(i)} + I_3 \ddot{\psi}_x^{(i)} - (e_o a)^2 \left[ I_2 \left( \ddot{u}_{xx}^{(i)} + \frac{1}{R_i^2} \ddot{u}_{\theta\theta}^{(i)} \right) + I_3 \left( \ddot{\psi}_{xx}^{(i)} + \frac{1}{R_i^2} \ddot{\psi}_{x\theta\theta}^{(i)} \right) \right] \quad (12d)$$

$$k_{51}^{(i)} u^{(i)} + k_{52}^{(i)} v^{(i)} + k_{53}^{(i)} w^{(i)} + k_{54}^{(i)} \psi_x^{(i)} + k_{55}^{(i)} \psi_\theta^{(i)} = I_2 \ddot{v}^{(i)} + I_3 \ddot{\psi}_\theta^{(i)} - (e_o a)^2 \left[ I_2 \left( \ddot{v}_{xx}^{(i)} + \frac{1}{R_i^2} \ddot{v}_{\theta\theta}^{(i)} \right) + I_3 \left( \ddot{\psi}_{\theta xx}^{(i)} + \frac{1}{R_i^2} \ddot{\psi}_{\theta\theta}^{(i)} \right) \right] \quad (12e)$$

For  $i=1,2$ . Differential operators written above are given in Appendix.

### 3. Application of wave propagation approach

Numerous methods and techniques have been employed

to get solution of differential equations and especially numerical solution always have been of great interest of researchers for advance research. The wave propagation first ever used by (Zhang *et al.* 2001) is an appropriate technique to investigate the vibration phenomena. This technique has been effectively exercised in determination of vibration spectra of shell/tube. Over the past several years vibration of tube structures of various configurations and boundary conditions have been extensively studied (Asghar *et al.* 2019a, b, Hussain *et al.* 2019, Hussain *et al.* 2018a, Hussain and Naeem 2018a, Hussain *et al.* 2018b, Hussain *et al.* 2018c, Sharma *et al.* 2019, Fatahi-Vajari *et al.* 2019). The shell modal displacement expressions with respect to wave propagation for  $i$ th tube are written as follow

$$u^{(i)}(x, \theta, t) = a_m \cos(n\theta) e^{(j\omega t - jk_m x)} \quad (13a)$$

$$v^{(i)}(x, \theta, t) = b_m \sin(n\theta) e^{(j\omega t - jk_m x)} \quad (13b)$$

$$w^{(i)}(x, \theta, t) = c_m \cos(n\theta) e^{(j\omega t - jk_m x)} \quad (13c)$$

$$\psi_x^{(i)}(x, \theta, t) = d_m \cos(n\theta) e^{(j\omega t - jk_m x)} \quad (13d)$$

$$\psi_\theta^{(i)}(x, \theta, t) = e_m \sin(n\theta) e^{(j\omega t - jk_m x)} \quad (13e)$$

In which  $a_m, b_m, c_m$  define the displacement amplitude sequentially in  $x, \theta$  and  $z$  directions. The angular frequency is denoted by  $\omega$ , circumferential wave number by  $n$  and  $k_m$  regarded as axial wave number conjoin with end supports imposed on double-walled CNTs. Substituting the derivatives and respective functions into the stated equations, hence obtained a new set of simultaneous equations as follows

$$K_{11}^{(i)} a_m^{(i)} + K_{12}^{(i)} b_m^{(i)} + K_{13}^{(i)} c_m^{(i)} + K_{14}^{(i)} d_m^{(i)} + K_{15}^{(i)} e_m^{(i)} = -\omega^2 (1 - (e_o a)^2 \nabla^2) [I_1 a_m^{(i)} + I_2 d_m^{(i)}] \quad (14a)$$

$$K_{21}^{(i)} a_m^{(i)} + K_{22}^{(i)} b_m^{(i)} + K_{23}^{(i)} c_m^{(i)} + K_{24}^{(i)} d_m^{(i)} + K_{25}^{(i)} e_m^{(i)} = -\omega^2 (1 - (e_o a)^2 \nabla^2) [I_1 b_m^{(i)} + I_2 e_m^{(i)}] \quad (14b)$$

$$K_{31}^{(i)} a_m^{(i)} + K_{32}^{(i)} b_m^{(i)} + K_{33}^{(i)} c_m^{(i)} + K_{34}^{(i)} d_m^{(i)} + K_{35}^{(i)} e_m^{(i)} + (1 - (e_o a)^2 \nabla^2) \left[ \sum_{j=1}^2 c_{ij} c_m^{(j)} - \sum_{j=1}^2 c_{ij} c_m^{(i)} \right] = -\omega^2 (1 - (e_o a)^2 \nabla^2) [I_1 c_m^{(i)}] \quad (14c)$$

$$K_{41}^{(i)} a_m^{(i)} + K_{42}^{(i)} b_m^{(i)} + K_{43}^{(i)} c_m^{(i)} + K_{44}^{(i)} d_m^{(i)} + K_{45}^{(i)} e_m^{(i)} = -\omega^2 (1 - (e_o a)^2 \nabla^2) [I_2 a_m^{(i)} + I_3 d_m^{(i)}] \quad (14d)$$

$$K_{51}^{(i)} a_m^{(i)} + K_{52}^{(i)} b_m^{(i)} + K_{53}^{(i)} c_m^{(i)} + K_{54}^{(i)} d_m^{(i)} + K_{55}^{(i)} e_m^{(i)} = -\omega^2 (1 - (e_o a)^2 \nabla^2) [I_2 b_m^{(i)} + I_3 e_m^{(i)}] \quad (14e)$$

( $i=1,2$ )

Where algebraic operators  $K_{ij}$ 's are written in Appendix.

The above equations are arranged as eigen value problem, and expressed in form of matrix to determine vibration analysis of double-walled CNTs based on nonlocal DSM using wave propagation approach.

$$\begin{bmatrix} K_{11} & K_{12} & K_{13} & K_{14} & K_{15} \\ K_{21} & K_{22} & K_{23} & K_{24} & K_{25} \\ K_{31} & K_{32} & K_{33} & K_{34} & K_{35} \\ K_{41} & K_{42} & K_{43} & K_{44} & K_{45} \\ K_{51} & K_{52} & K_{53} & K_{54} & K_{55} \end{bmatrix} \begin{bmatrix} a_m^{(i)} \\ b_m^{(i)} \\ c_m^{(i)} \\ d_m^{(i)} \\ e_m^{(i)} \end{bmatrix} = -\omega^2 S \begin{bmatrix} I_1 & 0 & 0 & 0 & 0 \\ 0 & I_1 & 0 & 0 & 0 \\ 0 & 0 & I_1 & 0 & 0 \\ 0 & 0 & 0 & I_3 & 0 \\ 0 & 0 & 0 & 0 & I_3 \end{bmatrix} \begin{bmatrix} a_m^{(i)} \\ b_m^{(i)} \\ c_m^{(i)} \\ d_m^{(i)} \\ e_m^{(i)} \end{bmatrix} \quad (15)$$

Table 1 Non dimensional results comparison with present results

Method	$e_0a$				
	0	1	2	3	4
Reddy (2007)	9.8696	8.983	8.2426	7.6149	47.0761
Aydogdu (2009)	9.8696	9.6319	9.4055	9.1894	8.983
Eltaher (2013)	9.86973	8.98312	8.24267	7.61499	7.07614
Karami <i>et al.</i> (2019)	9.80601	8.92692	8.19176	7.56846	7.03246
Present	9.80601	8.92692	8.19176	7.56846	7.03246

Table 2 Presenting the lower frequency ratio comparison for diverse indices of zigzag and chiral against aspect ratios ( $L/d$ ) when scale coefficient ( $e_0a$ ) is 2 nm

	Indices Zigzag		Indices Chiral		
	Rakrak <i>et al.</i> (2016)	Present	Rakrak <i>et al.</i> (2016)	Present	
(14, 0)	0.94169	0.94169	(12, 6)	0.94964	0.94964
(17, 0)	0.95365	0.95365	(14, 6)	0.82448	0.82448
(21, 0)	0.9647	0.9647	(16, 8)	0.95618	0.95618
(24, 0)	0.97062	0.97062	(18, 9)	0.96508	0.96508
(18, 0)	0.97647	0.97647	(20, 12)	0.97029	0.97029
(31, 0)	0.97979	0.97979	(24, 11)	0.97648	0.97648

The operators  $K_{ij}$ 's are already mentioned ones and  $S$  is also labeled in Appendix. The fundamental frequencies of double-walled CNTs are determined by eigen values and eigen vector is displayed as  $[a_m \ b_m \ c_m \ d_m \ e_m]^T$ .

#### 4. Results and discussions

On the basis of established nonlocal DSM by practicing with wave propagation approach, the dominance of end conditions of double-walled CNTs is presented. Sundry studies can be seen for authentic application of present technique to conclude governing equation system of CNTs and to examine the fundamental frequency of double-walled CNTs (Wang *et al.* 2006, Xu *et al.* 2008, Rouhi *et al.* 2011, Ansari *et al.* 2013). The procedure proposed in the previous section is here applied to study the size-dependent vibration behavior double-walled CNTs. Wave propagation approach is applied to form the presented model, whereby the size-dependent effect is considered by means of the application of the Eringen's nonlocal differential model. Thus, the vibration phenomena of the nanostructure are solved mathematically via the suggested approach for different boundary conditions. The parametric study presented in this work analyzes the sensitivity of the size-dependent vibration response of double-walled CNTs subjected to mechanical parameter (i.e., the nonlocal parameter), as well as to some geometrical parameters namely, the length, radius and height. The preliminary focus of the investigation is on the precision of the proposed technique with existing model, whose results are summarized in Table 1 in nondimensional form for an S-S condition, while varying the nonlocal parameter  $e_0a$ . Based on a comparative evaluation between our predictions and those obtained by

Table 3 Comparative estimate of natural frequency with the experimental results of Resonant Raman Spectroscopy (RRS)

$(m, n)$	$f$ (THz)			
	Zigzag		Chiral	
	(18, 0)	(21, 0)	(16, 7)	(18, 6)
RRS (Jorio <i>et al.</i> 2001)	5.276	4.437	4.617	4.317
Present	5.025	4.437	4.617	4.317
Difference %	4.76	3.74	4.85	4.04

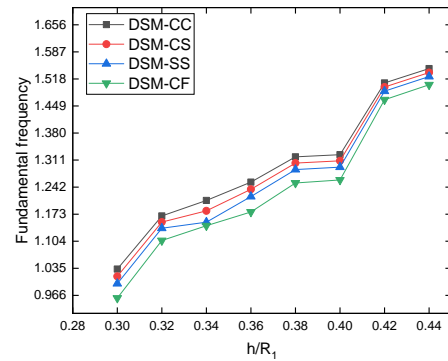


Fig. 2(a) Fundamental frequency for chiral (11, 2) against  $h/R_1$  with  $e_0a=0.45$

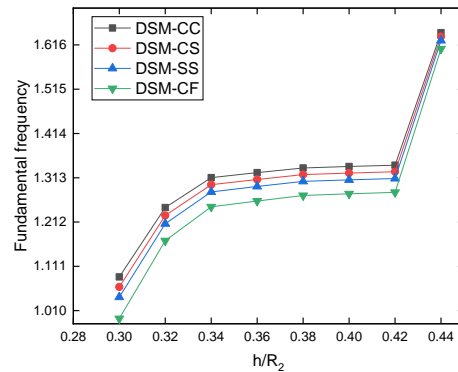


Fig. 2(b) Fundamental frequency for chiral (11, 2) against  $h/R_2$  with  $e_0a=0.45$

Reddy (2009), Aydogdu (2009), Eltaher (2013), Karami *et al.* (2019) a very good match was observed, which confirms the accuracy of the proposed formulation for similar problems. The influence of aspect ratio on zigzag and chirality are discussed in the Table 2. For comparison, various chiral and zigzag indices against distinct length-to-diameter ratios determined by the non-local Euler Bernoulli beam model are recorded in Table 2. For the current work the non-dimensional frequency parameters are also calculated to evaluate convergence rate of end supports of both chiral and zigzag double-walled CNTs. The results generated by present model solved with wave propagation approach seen to have accordance with those experimental outputs of Jorio *et al.* (2001) obtained by the deformation theory are specified in Table 3. The results obtained here specifically deal with the small scale effect versus length and thickness to radius of both tubes. For the purpose of numerical computations estimates of Young's modulus and

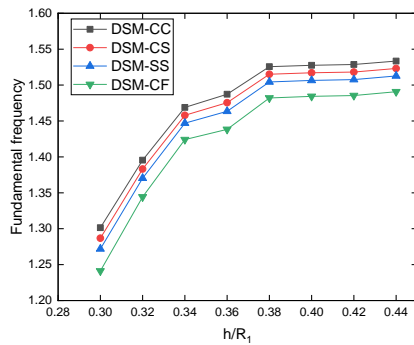


Fig. 3(a) Fundamental frequency for chiral (15, 2) against  $h/R_1$  with  $e_0a=0.45$

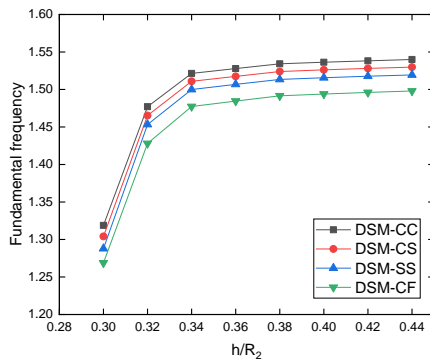


Fig. 3(b) Fundamental frequency for chiral (15, 2) against  $h/R_2$  with  $e_0a=0.45$

Poisson's ratio are  $E=1$  TPA,  $\rho=2.3$  g/cm<sup>3</sup> remain unchanged as used (Rouhi *et al.* 2011).

Furthermore, inner tube radius  $R_1=8.5$  nm and thickness to radius ratio are observed along with calibrated values of nonlocal parameter. Carbon nanotubes structure exhibit in forms as i) armchair, ii) zigzag, iii) chiral, for the ongoing investigation of vibration spectra of chiral and zigzag CNT based on DSM are demonstrated together with end supports clamped-clamped (DSM-CC), clamped-simply supported (DSM-CS), simply supported-simply supported (DSM-SS) and clamped-free (DSM-CF). Graphs 2(a) and 2(b) are frequency depiction of chiral double-walled CNTs with indices (11, 2) versus thickness-to-radius ratio and range of effective thickness varies from 0.32 nm to 0.44 nm. It exhibits the comparison for aspect ratio with respect to both inner and outer tubes radii. In both Fig. 2(a) and 2(b) the inner radius  $R_1=8.5$  nm and  $e_0a=0.45$  nm are considered for the all end supports whereas the length of tube remains fixed. It is obvious from the first Fig. 2(a) that frequency curve moves up like a ladder as the aspect ratio along inner tube increases. Frequency value of end condition clamped-clamped (DSM-CC) is higher followed by (DSM-CS), (DSM-SS) and (DSM-CF). The influence of boundary conditions is more pronounced in the first Fig. 2(a) between the range 0.30 nm and 0.40 nm of aspect ratio. After that curve has a jump at 0.42 nm and difference between end conditions diminishes as thickness-to-radius continue to increase. Fig. 2(b) shows the higher values of frequencies when aspect ratio is taken along the outer tube radius. It is observed from the 2(b) as thickness-to-radius ratio

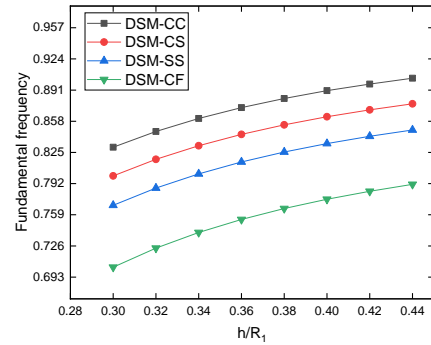


Fig. 4(a) Fundamental frequency for zigzag double (7, 0) against  $h/R_1$  with  $e_0a=0.45$

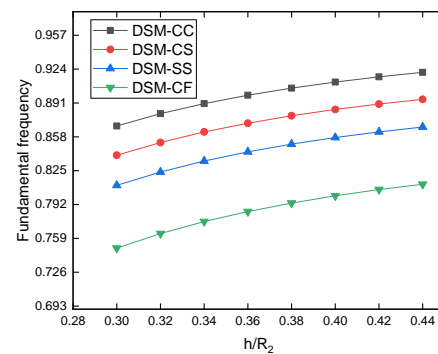


Fig. 4(b) Fundamental frequency for zigzag (7, 0) against  $h/R_2$  with  $e_0a=0.45$

increases, respective frequencies for all end conditions tend to increase.

A leap again is seen in curve as aspect ratio hits at 0.42 nm but with this the minute difference between end conditions recede. Another observation is realized that frequency results exceed for aspect ratio  $h/R$  as compare to  $h/R_1$ . The curves in 3(a) and 3(b) are frequencies with nonlocal parameter  $e_0a=0.45$  for chiral double-walled CNTs with indices (15, 2) versus thickness -to-radius ratio. The other parameters remain same for these calculations. The frequencies are displaying increasing pattern with an increase in indices of chiral double-walled CNTs, as (11, 2) exhibited less values of frequencies, whereas (15, 2) have shown the higher frequencies. The boundary condition (DSM-CF) is at a minor difference from the other three conditions, on the other hand (DSM-CC), (DSM-CS) and (DSM-SS) possess the less difference. So, as indices increase for chiral double-walled CNTs the respective frequency also increases. The same behaviour is noticed for both aspect ratios as for aspect ratio  $h/R_2$  frequencies are followed by  $h/R_1$ . The graphs 4(a) and 4(b) represent zigzag double-walled CNTs with indices (7, 0) against both aspect ratios  $h/R_1$  and  $h/R_2$ . The Fig. 5(a) and 5(b) portray the zigzag double-walled CNTs along with indices (12, 0) versus aspect ratios corresponding to both tubes radii. The value for nonlocal parameter  $e_0a=0.45$  nm is considered and length of tube to be fixed. In all above graphs the pattern is observed alike, but on inspecting them keenly two facts are noticed. One as increasing pattern is displayed subjected to all end supports but as aspect ratio keeps on increasing the

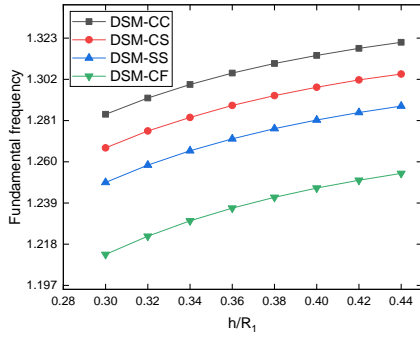


Fig. 5(a) Fundamental frequency for zigzag (12, 0) against  $h/R_1$  with  $e_0a=0.45$

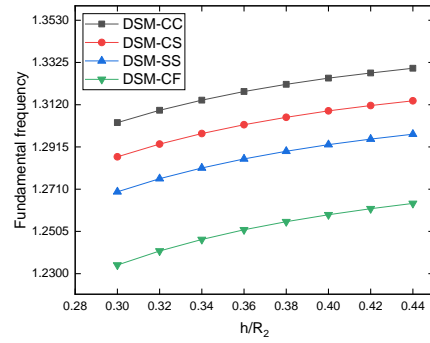


Fig. 5(b) Fundamental frequency for zigzag (12, 0) against  $h/R_2$  with  $e_0a=0.45$

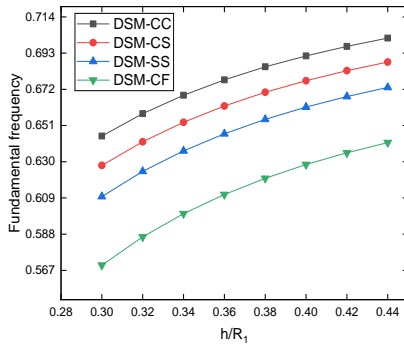


Fig. 6(a) Fundamental frequency for zigzag (7, 0) against  $h/R_1$  with  $e_0a=0.90$

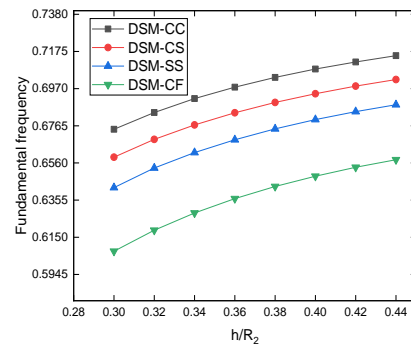


Fig. 6(b) Fundamental frequency for zigzag (7, 0) against  $h/R_2$  with  $e_0a=0.90$

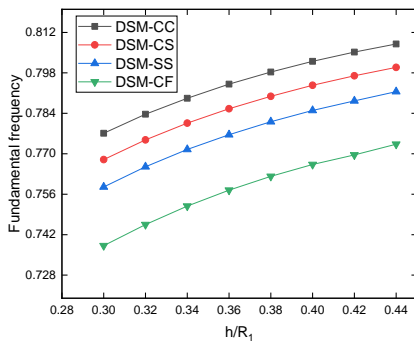


Fig. 7(a) Fundamental frequency for zigzag (12, 0) against  $h/R_1$  with  $e_0a=0.90$

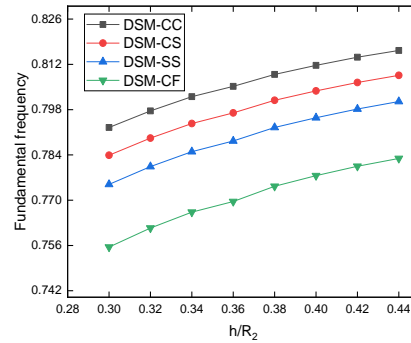


Fig. 7(b) Fundamental frequency for zigzag (12, 0) against  $h/R_2$  with  $e_0a=0.90$

natural frequencies start to show less increase and get more parallel to each other. That means after a certain increase in range of aspect ratio the frequency begin to produce more repeated /close results. Secondly the validation of the model DSM is reflected by these curves as zigzag (7, 0) shows lowest frequencies than those of zigzag (12, 0). Similarly  $h/R_2$  possess the higher natural frequencies for zigzag (7, 0) and (12, 0) double-walled CNTs. The end supports (DSM-CS) and (DSM-SS) are sandwich between (DSM-CC) and (DSM-CF).

The Figs. 6(a), 6(b), 7(a) and 7(b) are plotted above for zigzag double-walled CNTs (7, 0) and (12, 0) with nonlocal parameter  $e_0a=0.90$ . It is seen that with an increase in scale effect value the frequencies depending upon four boundary conditions tend to decrease in a comparison of  $e_0a=0.90$  against thickness-to-radius ratio. However, the pattern

demonstrates the identical behaviour of increase in fundamental frequencies as an increase in aspect ratio. Hence the nonlocal parameter scales down the natural frequencies with an increase in it. Further, in next graphs the domination of end supports on free vibrations of double-walled CNTs is demonstrated via length -to- diameter ratio. The other numerical estimates remain fixed along with distinct values of nonlocal parameter. The fundamental frequencies are analyzed for specifically zigzag and chiral double-walled CNTs. The executed outcomes confirm the appropriate utilization of nonlocal DSM with the suggested wave propagation approach. The Fig. 8(a) and 8(b) are illustrations of zigzag double walled CNTs with indices (7, 0). In these graphs the significance of end supports have been displayed for zigzag double-walled CNT corresponding to two values of nonlocal parameters

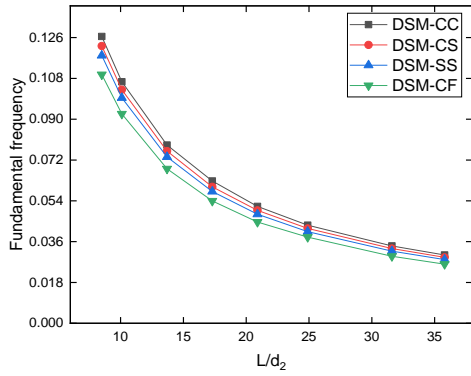


Fig. 8(a) Fundamental frequency for zigzag (7,0) against  $L/d_2$  with  $e_0a=0.45$

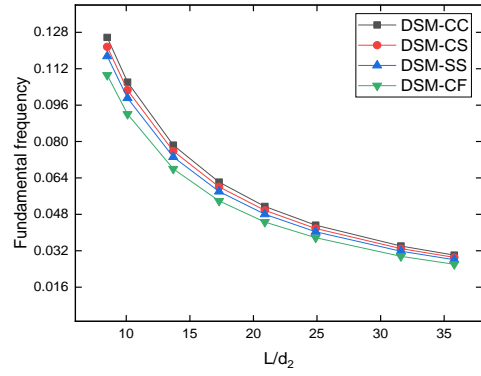


Fig. 8(b) Fundamental frequency for zigzag (7,0) against  $L/d_2$  with  $e_0a=0.90$

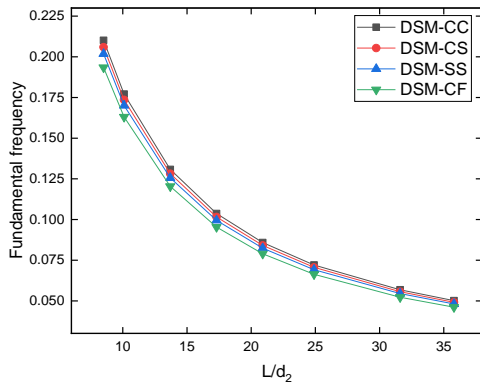


Fig. 9(a) Fundamental frequency for zigzag (12, 0) against  $L/d_2$  with  $e_0a=0.45$

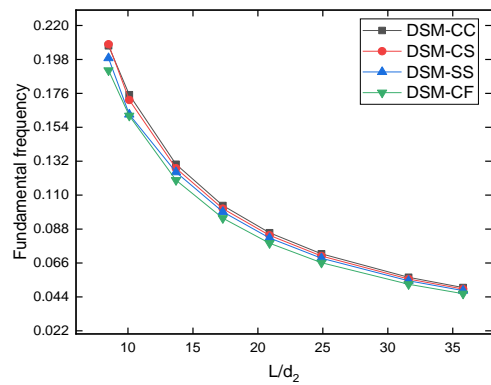


Fig. 9(b) Fundamental frequency for zigzag (12, 0) against  $L/d_2$  with  $e_0a=0.90$

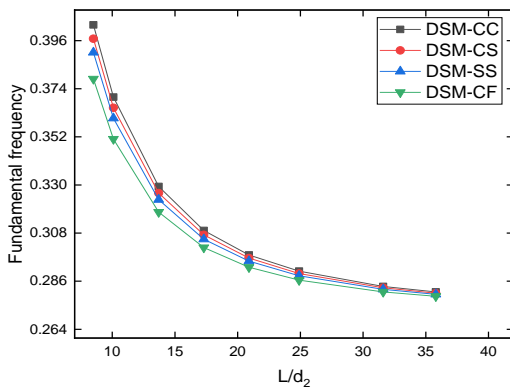


Fig. 10(a) Fundamental frequency for chiral double-walled CNT (11, 2) against  $L/d_2$  with  $e_0a=0.45$ .

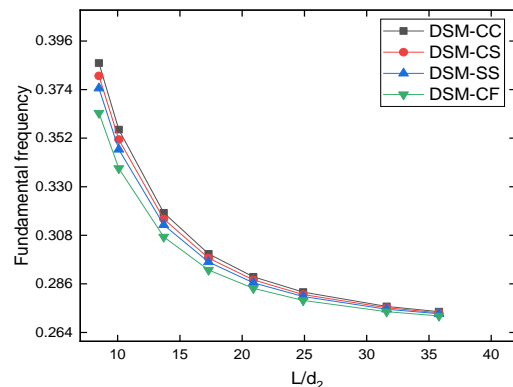


Fig. 10(b) Fundamental frequency for chiral double-walled CNT (11, 2) against  $L/d_2$  with  $e_0a=0.90$ .

$e_0a=0.45, 0.90$ . The fundamental frequencies are calculated against length to diameter ratio, ranges from 8.3 to 35.8 (Ansari). The frequency of zigzag (7, 0) with  $e_0a=0.90$  shows low values on curves, whereas the frequency versus  $e_0a=0.45$  observe the highest values on comparison. The difference among the four end supports in both figures is more evidently shown in the beginning. In Fig. 9(a) and 9(b), fundamental frequencies are examined for zigzag (12, 0) double-walled CNTs against  $e_0a=0.45, 0.90$  along with aspect ratio  $L/d_2$ . The response and pattern of frequency curves are analogous. However, the frequency is declining with an increase in indices of zigzag double-walled CNTs.

This is how it shows a reasonable correlation with (Ansari *et al.* 2013). It is a matter of concern to calibrate the precise value of nonlocal parameter to predict the natural frequencies for CNTs. As  $L/d_2$  expands, frequencies portray a decline in curves and all curves almost meet at end for four end supports. The Fig. 10(a) and 10(b) are frequency curves of chiral double-walled CNTs with indices (11,2), on the other hand 11(a) and 11(b) show the frequency graphs of (9, 4) chiral double-walled CNTs. In 10(a) and 11(a) the calculated natural frequencies are shown against  $e_0a=0.45$  and aspect ratio  $L/d_2$ , however for 10(b) and 11(b) versus  $e_0a=0.90$ . The aspect ratio  $L/d_2$  ranges from 13.7 to 39.5 for

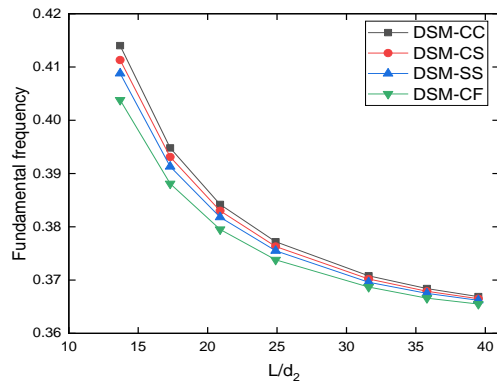


Fig. 11(a) Fundamental frequency for chiral (9, 4) against  $L/d_2$  with  $e_0a=0.45$

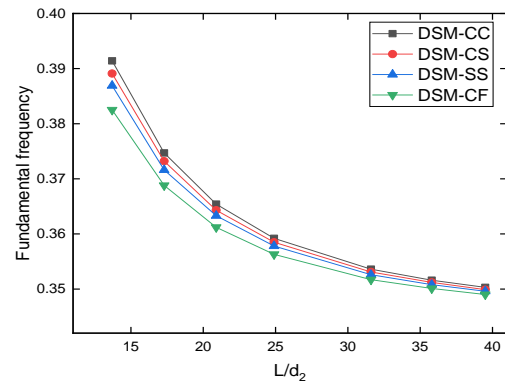


Fig. 11(b) Fundamental frequency for chiral (9, 4) against  $L/d_2$  with  $e_0a=0.90$

these four graphs subjected to clamped-clamped (DSM-CC), clamped supported (DSM-CS), simply supported-simply supported (DSM-SS) and clamped-free (DSM-CF). The natural frequency via aspect ratio  $L/d_2$  descends as length-to-diameter expands subjected to all end supports. The difference between the conditions is obvious in beginning and vanishes as length of tube continues to extend. This behaviour and trend of curves reflects the fact that scale effect becomes negligible for longer tubes and also as scale rises the frequency declines for all end supports. The frequency for chiral (9, 4) attains increasing frequency pattern over the chiral (8, 3) as the previous zigzag and chiral double-walled CNTs have been observed

## 5. Conclusion

The free vibration analysis of chiral and zigzag double-walled CNTs is presented based on nonlocal DSM by exercising wave propagation approach. Influence of four end supports against length-to-diameter ratio and thickness-to-radius ratio with varying nonlocal parameter are discussed and shown graphically. The fundamental frequency curves displayed in article show the dependence of vibration attributes on the chiral and zigzag double-walled CNT with regard to nonlocal parameter. Different indices are considered against aspect ratio to show the diversity of vibration characteristic of chiral and zigzag. According to the results, it is found that nonlocal effect is more prominent in increasing length of tubes for both chiral and zigzag double-walled CNTs. The aspect ratio thickness-to-radius are compared with both radii, it is observed that  $h/R_1$  show the lowest frequency as compare to  $h/R_2$ . The fundamental frequency curves show an increasing pattern as indices of chiral and zigzag observe an increase. Also it is examined that if thickness- to -radius ratio expands, the frequency tend to increase too within specified range. In addition as length- to- diameter ratio increases the difference between end supports become negligible and meet all curves at end for respective four end conditions. The nonlocal parameter value with an increase show the reduced frequency for both chiral and zigzag. The adoption of wave propagation method sustain the fact that nonlocal effect is insignificant for longer carbon nanotubes and can

be engage effectively for further work on double-walled CNTs and multi-walled CNTs.

## Declaration of conflicting interests

The author(s) declared no potential conflicts of interest with respect to the research, authorship, and/or publication of this article.

## Funding

The author(s) received no financial support for the research, authorship, and/or publication of this article.

## References

- Ansari, R. and Rouhi, H. (2012), "Nonlocal analytical Flugge shell model for the axial buckling of double-walled carbon nanotubes with different end conditions", *Int. J. Nano Dimens.*, **7**(3), 1250081. <https://doi.org/10.1142/S179329201250018X>.
- Ansari, R., Rouhi, H. and Arash, B. (2013), "Vibration analysis of double-walled carbon nanotubes based on the nonlocal donnell shell via a new numerical approach", *Int. J. Sci. Technol. Tran. B: Eng.*, **37**, 91-105.
- Asghar, S., Hussain, M. and Naeem, M. (2019a), "Non-local effect on the vibration analysis of double walled carbon nanotubes based on Donnell shell theory", *Physica E: Low Dimens. Syst. Nanostr.*, **116**, 113726. <https://doi.org/10.1016/j.physe.2019.113726>.
- Asghar, S., Hussain, M. and Naeem, M.N. (2019b), "Non-local effect on the vibration analysis of double walled carbon nanotubes based on Donnell shell theory", *Physica E: Low Dimens. Syst. Nanostr.*, **116**, 11326. <https://doi.org/10.1016/j.physe.2019.113726>.
- Avcar, M. (2019), "Free vibration of imperfect sigmoid and power law functionally graded beams", *Steel Compos. Struct.*, **30**(6), 603-615. <https://doi.org/10.12989/scs.2019.30.6.603>.
- Aydogdu, M. (2009), "A general nonlocal beam theory: Its application to nanobeam bending, buckling and vibration", *Physica E*, **41**, 1651-1655. <https://doi.org/10.1016/j.physe.2009.05.014>.
- Batou, B., Nebab, M., Bennai, R., Atmane, H.A., Tounsi, A. and Bouremana, M. (2019), "Wave dispersion properties in imperfect sigmoid plates using various HSDTs", *Steel Compos. Struct.*, **33**(5), 699-716. <https://doi.org/10.12989/scs.2019.33.5.699>.

- Benguediab, S., Tounsi, A., Zidour, M. and Semmah, A. (2014), "Chirality and scale effects on mechanical buckling properties of zigzag double-walled carbon nanotubes", *Compos. Part B: Eng.*, **57**, 21-24. <https://doi.org/10.1016/j.compositesb.2013.08.020>.
- Bisen, H.B., Hirwani, C.K., Satankar, R.K., Panda, S.K., Mehar, K. and Patel, B. (2018), "Numerical study of frequency and deflection responses of natural fiber (Luffa) reinforced polymer composite and experimental validation", *J. Nat. Fib.*, 1-15. <https://doi.org/10.1080/15440478.2018.1503129>.
- Bouazza, M., Amara, K., Zidour, M., Tounsi, A. and El Abbas, A.B. (2014), "Thermal effect on buckling of multiwalled carbon nanotubes using different gradient elasticity theories", *Nanosci. Nanotechnol.*, **4**(2) 27-33. <https://doi.org/10.5923/j.nn.20140402.02>.
- Brischetto, S. (2014), "A continuum elastic three-dimensional model for natural frequencies of single walled carbon nanotubes", *Compos. Part B: Eng.*, **61**, 222-228. <https://doi.org/10.1016/j.compositesb.2014.01.046>.
- Chang, T., Li, G. and Gua, X. (2005), "Elastic axial buckling of carbon nanotubes via molecular mechanics model", *Carbon*, **43**, 287-294. <https://doi.org/10.1016/j.carbon.2004.09.012>.
- Chang, W.J. and Lee, H.L. (2009), "Free vibration of single-walled carbon nanotubes containing a fluid flow using a Timoshenko beam model", *Phys. Lett. A*, **373**(10), 982-985. <https://doi.org/10.1016/j.physleta.2009.01.011>.
- Chemi, A., Heireche, H., Zidour, M., Rakrak, K. and Bousahla, A.A. (2015), "Critical buckling load chiral double-walled carbon nanotubes using non-local elasticity theory", *Adv. Neno Res.*, **3**(4), 193-206. <https://doi.org/10.12989/anr.2015.3.4.193>.
- Cornwell, C.F. and Wille, L.T. (1997), "Elastic properties of single-walled carbon nanotubes in compression", *Solid State Commun.*, **101**(8), 555-558. [https://doi.org/10.1016/S0038-1098\(96\)00742-9](https://doi.org/10.1016/S0038-1098(96)00742-9).
- Ebrahimi, F., Barati, M.R. and Mahesh, V. (2019), "Dynamic modeling of smart magneto-electro-elastic curved nanobeams", *Adv. Nano Res.*, **7**(3), 145-155. <https://doi.org/10.12989/anr.2019.7.3.145>.
- Eltaher, M., Emam, S.A. and Mahmoud, F. (2013), "Static and stability analysis of nonlocal functionally graded nanobeams", *Compos. Struct.*, **96**, 82-88. <https://doi.org/10.1016/j.compstruct.2012.09.030>.
- Eltaher, M.A., Eman, S.A. and Mahmoud, F.F. (2013), "Static and stability analysis of nonlocal functionally graded nanobeams", *Compos. Struct.*, **96**, 82-88. <https://doi.org/10.1016/j.compstruct.2012.09.030>.
- Eringen, A.C. (1972), "Nonlocal polar elastic continua", *Int. J. Eng. Sci.*, **10**(1), 1-16. [https://doi.org/10.1016/0020-7225\(72\)90070-5](https://doi.org/10.1016/0020-7225(72)90070-5).
- Eringen, A.C. (1983), "On differential equations of nonlocal elasticity and solutions of screw dislocation and surface waves", *J. Appl. Phys.*, **54**, 4703-4710. <https://doi.org/10.1063/1.332803>.
- Eringen, A.C. (2002), *Nonlocal Continuum Field Theories*, Springer Science and Business Media, New York.
- Fatahi-Vajari, A., Azimzadeh, Z. and Hussain, M. (2019), "Nonlinear coupled axial-torsional vibration of single-walled carbon nanotubes using Galerkin and Homotopy perturbation method", *Micro Nano Lett.*, **14**(14), 1366-1371. <https://doi.org/10.1049/mnl.2019.0203>.
- Ghavanloo, E. and Fazelzadeh, S.A. (2009), "Vibrations characteristics of single walled carbon nanotubes based on the nonlocal Flugge shell theory". *ASME J. Eng. Mater. Technol.*, **134**, 011008. <https://doi.org/10.1016/j.apm.2011.12.036>.
- Gohardani, O., Elola, M.C. and Elizetxea, C. (2014), "Potential and prospective implementation of carbon nanotubes on next generation aircraft and space vehicle: A review of current and expected applications in aerospace sciences", *Prog. Aerosp. Sci.*, **70**, 42-68. <https://doi.org/10.1016/j.paerosci.2014.05.002>.
- Hao, X., Qiang, H. and Xiaouh, Y. (2008), "Buckling of defective single-walled and double-walled carbon nanotubes under axial compression by molecular dynamic simulation", *Compos. Sci. Technol.*, **68**(7-8), 1809-1814. <https://doi.org/10.1016/j.compscitech.2008.01.013>.
- Hashemi, S.H., Ilkhani, M.R. and Fadaee, M. (2012), "Identification of the validity of the Donnell and Sanders shell theories using an exact vibration analysis of the functionally graded thick cylindrical shell panel", *Acta Mechanica*, **223**(5), 1101-1118. <https://doi.org/10.1007/s00707-011-0601-0>.
- Heireche, H., Tounsi, A., Benzair, A., Maachou, M. and AddaBedia, E.A. (2008), "Sound wave propagation in single-walled carbon nanotubes using nonlocal elasticity", *Physica E: Low Dimens. Syst. Nanostr.*, **40**(8), 2791-2799. <https://doi.org/10.1016/j.physe.2007.12.021>.
- Hu, Y.G., Liew, K.M. and Wang, Q. (2012), "Modeling of vibrations of carbon nanotubes", *Procedia Eng.*, **31**, 343-347. <https://doi.org/10.1016/j.proeng.2012.01.1034>.
- Hu, Y.G., Liew, K.M. and Wang, Q. (2012), "Modeling of vibrations of carbon nanotubes", *Procedia Eng.*, **31**, 343-347. <https://doi.org/10.1016/j.proeng.2012.01.1034>.
- Hu, Y.G., Liew, K.M., Wang, Q., He, X.Q. and Yakobson, B.I. (2008), "Nonlocal shell model for elastic wave propagation in single- and double-walled carbon nanotubes", *J. Mech. Phys. Solid.*, **56**(12), 3475-3485. <https://doi.org/10.1016/j.jmps.2008.08.010>.
- Hussain, M. and Naeem, M. (2018b), "Vibration of single-walled carbon nanotubes based on Donnell shell theory using wave propagation approach", *Novel Nanomater. Synth. Appl.*, **18**, 77. <https://doi.org/10.5772/intechopen.73503>.
- Hussain, M. and Naeem, M. (2019c), "Rotating response on the vibrations of functionally graded zigzag and chiral single walled carbon nanotubes", *Appl. Math. Model.*, **75**, 506-520. <https://doi.org/10.1016/j.apm.2019.05.039>.
- Hussain, M. and Naeem, M.N. (2017), "Vibration analysis of single-walled carbon nanotubes using wave propagation approach", *Mech. Sci.*, **8**(1), 155-164. <https://doi.org/10.5194/ms-8-155-2017>.
- Hussain, M. and Naeem, M.N. (2018a), "Effect of various edge conditions on free vibration characteristics of rectangular plates", *Advance Testing and Engineering*.
- Hussain, M. and Naeem, M.N. (2019), "Vibration characteristics of single-walled carbon nanotubes based on nonlocal elasticity theory using Wave Propagation Approach (WPA) Including Chirality", *Perspective of Carbon Nanotubes*. <http://dx.doi.org/10.5772/intechopen.85948>.
- Hussain, M. and Naeem, M.N. (2019a), "Effects of ring supports on vibration of armchair and zigzag FGM rotating carbon nanotubes using Galerkin's method", *Compos. Part B. Eng.*, **163**, 548-561. <https://doi.org/10.1016/j.compositesb.2018.12.144>.
- Hussain, M. and Naeem, M.N. (2019b), "Vibration characteristics of zigzag and chiral FGM rotating carbon nanotubes sandwich with ring supports", *J. Mech. Eng. Sci., Part C*, **233**(16), 5763-5780. <https://doi.org/10.1177/0954406219855095>.
- Hussain, M., Naeem, M., Shahzad, A. and He, M. (2018a), "Vibration characteristics of fluid-filled functionally graded cylindrical material with ring supports", *Comput Fluid Dyn Basic Instrum Appl Sci.*, 333. <https://doi.org/10.5772/intechopen.72172>.
- Hussain, M., Naeem, M.N. and Isvandzibaei, M. (2018c), "Effect of Winkler and Pasternak elastic foundation on the vibration of rotating functionally graded material cylindrical shell", *Proc. Inst. Mech. Eng., Part C: J. Mech. Eng. Sci.*, **232**(24), 4564-4577. <https://doi.org/10.1177/0954406217753459>.
- Hussain, M., Naeem, M.N. and Taj, M. (2019b), "Effect of length and thickness variations on the vibration of SWCNTs based on Flugge's shell model", *Micro Nano Lett.*, **15**(1), 1-6. <https://doi.org/10.1049/mnl.2019.0309>, 2019.
- Hussain, M., Naeem, M.N., Shahzad, A., He, M. and Habib, S.

- (2018b), "Vibrations of rotating cylindrical shells with FGM using wave propagation approach", *IMechE Part C: J. Mech. Eng. Sci.*, **232**(23), 4342-4356.
- Hussain, M., Naeem, M.N., Tounsi, A. and Taj, M. (2019a), "Nonlocal effect on the vibration of armchair and zigzag SWCNTs with bending rigidity", *Adv. Nano Res.*, **7**(6), 431. <https://doi.org/10.12989/anr.2019.7.6.431>.
- Hussain, M., Naeem, M.N., Tounsi, A. and Taj, M. (2020), "Simulating vibration of single-walled carbon nanotube using Rayleigh-Ritz's method", *Adv. Nano Res.*, **8**(3).
- Hussain, M., Naeem, M.N., Shahzad, A. and He, M. (2017), "Vibrational behavior of single-walled carbon nanotubes based on cylindrical shell model using wave propagation approach", *AIP Adv.*, **7**(4), 045114. <https://doi.org/10.1063/1.4979112>.
- Jamali, M., Shojae, T., Mohammadi, B. and Kolahchi, R. (2019), "Cut out effect on nonlinear post-buckling behavior of FG-CNTRC micro plate subjected to magnetic field via FSDT", *Adv. Nano Res.*, **7**(6), 405-417. <https://doi.org/10.12989/anr.2019.7.6.405>.
- Jorio, A., Saito, R., Hafner, J.H., Lieber, C.M., Hunter, M., McClure, T., Dresselhaus, G. and Dresselhaus, M.S. (2001), "Structural (n,m) determination of isolated single-wall carbon nanotubes by resonant raman scattering", *Phys. Rev. Lett.*, **86**(6) 1118-1121. <https://doi.org/10.1103/PhysRevLett.86.1118>.
- Jung, N.Y. and Han, S.C. (2013), "Analysis of sigmoid functionally materials (S-FGM) nanoscale plates using nonlocal elasticity theory", *Math. Prob. Eng.*, 476131. <http://dx.doi.org/10.1155/2013/476131>
- Karami, B., Janghorban, M., Shahsavari, D., Dimitri, R., & Tornabene, F. (2019), "Nonlocal buckling analysis of composite curved beams reinforced with functionally graded carbon nanotubes", *Molecul.*, **24**, 2750. <https://doi.org/10.3390/molecules24152750>.
- Kasas, S., Cibert, C., Kis, A., De Rios, P.L., Riederer, B.M., Forro, L., Dietler, G. and Catsicas, S. (2004), "Oscillation modes of microtubules", *Biology Cell*, **96**(9), 697-700. <https://doi.org/10.1016/j.biocel.2004.09.002>.
- Ke, L.L., Xiang, Y., Yang, J. and Kitipornchai, S. (2009), "Non linear free vibration of embedded double-walled carbon nanotubes based on nonlocal Timoshenko beam theory", *Comput. Mater. Sci.*, **47**(2), 409-417. <https://doi.org/10.1016/j.commatsci.2009.09.002>.
- Kolohchi, R., Bidholi, M.M. and Heydari, M.M. (2015), "Size-dependent bending analysis of FGM nano-sinusoidal plates resting on orthotropic elastic medium", *Struct. Eng. Mech.*, **55**, 1001-1014. <http://dx.doi.org/10.12989/sem.2015.55.5.1001>.
- Kostarelos, K., Bianco, A. and Prato, M. (2009), "Promises, facts and challenges for carbon nanotubes in imaging and therapeutics", *Nat. Nanotechnol.*, **4**(10), 627-633. <https://doi.org/10.1038/nnano.2009.241>.
- Lau, K.T. and Hui, D. (2002), "The revolutionary creation of new advanced materials-carbon nanotube composites", *Compos. Part B: Eng.*, **33**(4), 263-277. [https://doi.org/10.1016/S1359-8368\(02\)00012-4](https://doi.org/10.1016/S1359-8368(02)00012-4).
- Li, R. and Kardomateas, G.A. (2007) "Vibration characteristics of multiwalled carbon nanotubes embedded in elastic media by a nonlocal elastic shell model", *J. Appl. Mech.*, **74**(6), 1087-1094. <https://doi.org/10.1115/1.2722305>.
- Lieber, C.M. (2003), "Nanoscale science and technology building", *MRS Bulletin*. <https://doi.org/10.1557/mrs2003.144>.
- Liew, K.M., Wong, C.H., He, X.Q. and Tan, M.J. (2005), "Thermal stability of single and multi-walled carbon nanotubes", *Phys. Rev B*, **71**, 075424. <https://doi.org/10.1103/PhysRevB.71.075424>.
- Liu, L. and Zang, Y. (2004), "Multi-wall carbon nanotubes as a new infrared detected material", *Sens. Actu. A: Phys.*, **116**(3), 394-339. <https://doi.org/10.1016/j.sna.2004.05.016>.
- Lu, Y.J., Wang, X. and Lu, G. (2007), "Buckling of embedded multi-walled carbon nanotubes under combined torsion and axial loading", *Int. J. Solid. Struct.*, **44**(1), 336-351. <https://doi.org/10.1016/j.ijsolstr.2006.04.031>.
- Mehar, K. and Kumar Panda, S. (2018), "Thermal free vibration behavior of FG-CNT reinforced sandwich curved panel using finite element method", *Polym. Compos.*, **39**(8), 2751-2764. <https://doi.org/10.1002/pc.24266>.
- Mehar, K. and Panda, S.K. (2019), "Multiscale modeling approach for thermal buckling analysis of nanocomposite curved structure", *Adv. Nano Res.*, **7**(3), 181. <https://doi.org/10.12989/anr.2019.7.3.181>.
- Mehar, K., Mahapatra, T.R., Panda, S.K., Katariya, P.V. and Tompe, U.K. (2018), "Finite-element solution to nonlocal elasticity and scale effect on frequency behavior of shear deformable nanoplate structure", *J. Eng. Mech.*, **144**(9), 04018094. [https://doi.org/10.1061/\(ASCE\)EM.1943-7889.0001519](https://doi.org/10.1061/(ASCE)EM.1943-7889.0001519).
- Mehar, K., Panda, S.K. and Mahapatra, T.R. (2017a), "Thermoelastic nonlinear frequency analysis of CNT reinforced functionally graded sandwich structure", *Eur. J. Mech. A/Solid.*, **65**, 384-396. <https://doi.org/10.1016/j.euromechsol.2017.05.005>.
- Mehar, K., Panda, S.K. and Mahapatra, T.R. (2017b), "Theoretical and experimental investigation of vibration characteristic of carbon nanotube reinforced polymer composite structure", *Int. J. Mech. Sci.*, **133**, 319-329. <https://doi.org/10.1016/j.ijmecsci.2017.08.057>.
- Mehar, K., Panda, S.K. and Patle, B.K. (2018), "Stress, deflection, and frequency analysis of CNT reinforced graded sandwich plate under uniform and linear thermal environment: A finite element approach", *Polym. Compos.*, **39**(10), 3792-3809. <https://doi.org/10.1002/pc.24409>.
- Mehar, K., Panda, S.K., Dehengia, A. and Kar, V.R. (2016), "Vibration analysis of functionally graded carbon nanotube reinforced composite plate in thermal environment", *J. Sandw. Struct. Mater.*, **18**(2), 151-173. <https://doi.org/10.1177/1099636215613324>.
- Mori, H., Hirai, Y., Ogata, S., Akita, S. and Nakayama, Y. (2005), "Chirality dependence of mechanical properties of single walled carbon nanotubes under axial tensile strain", *JPN J. Appl. Phys.*, **44**(2), 42-45. <https://doi.org/10.1143/JJAP.44.L1307>.
- Mummmu, T. and Pradhan, S.C. (2010), "Thermal effects on the stability of embedded carbon nanotubes", *Comput. Mater. Sci.*, **47**(3), 721-726. <https://doi.org/10.1016/j.commatsci.2009.10.015>.
- Nejad, M.Z., Hadi, A. and Rastgoo, A. (2016), "Buckling analysis of arbitrary two-directional functionally graded Euler-Bernonllinano-beams based on non-local elasticity theory", *Eng. Sci.*, **103**, 1-10. <https://doi.org/10.1016/j.ijengsci.2016.03.001>.
- Nogales, E. (2001), "Structural insights into microtubule function", *Ann. Rev. Biophys. Biomol. Struct.*, **30**(1), 397-420. <https://doi.org/10.1146/annurev.biophys.30.1.397>.
- Pradhan, S.C. and Reddy, G.K. (2011), "Thermo mechanical buckling analysis of carbon nanotubes on Winkler foundation using non-local elasticity theory and DTM", *Sadhana*, **36**(6), 1009-1019. <https://doi.org/10.1007/s12046-011-0052-2>.
- Rafiee, R. and Moghadam, R.M. (2014), "On the modeling of carbon nanotubes: A critical review", *Compos. Part B: Eng.*, **56**, 435-449. <https://doi.org/10.1016/j.compositesb.2013.08.037>.
- Rakrak, K., Zidour, M., Heireche, H., Bousahla, A.A. and Chemi, A. (2016), "Free vibration analysis of chiral double-walled carbon nanotube using non-local elasticity theory", *Adv. Nano Res.*, **4**(1), 31-44. <http://dx.doi.org/10.12989/anr.2016.4.1.031>.
- Reddy, J.N. (2007), "Nonlocal theories for bending, buckling and vibration of beams", *Int. J. Eng. Sci.*, **45**, 288-307. <https://doi.org/10.1016/j.ijengsci.2007.04.004>.
- Regi, M. (2007), "6-synthesis, characteristics and applications of carbon nanotubes: the case of aerospace engineering", *Nanofib.*

- Nanotech. Textil.*, 113-193.  
<https://doi.org/10.1533/9781845693732.2.113>.
- Reilly, R.M. (2007), "Carbon nanotubes: Potential benefits and risks of nanotechnology in nuclear medicine", *J. Nucl. Med.*, **48**(7), 1039-1042. <http://doi.org/10.2967/jnumed.107.041723>.
- Salah, F., Boucham, B., Bourada, F., Benzair, A., Bousahla, A.A. and Tounsi, A. (2019), "Investigation of thermal buckling properties of ceramic-metal FGM sandwich plates using 2D integral plate model", *Steel Compos. Struct.*, **32**(5), 595-610. <https://doi.org/10.12989/scs.2019.33.6.805>.
- Sharma, P., Singh, R. and Hussain, M. (2019), "On modal analysis of axially functionally graded material beam under hygrothermal effect", *Proc. Inst. Mech. Eng., Part C: J. Mech. Eng. Sci.* 10.1177/0954406219888234, 2019.
- Soldano, C. (2015), "Hybrid metal-based carbon nanotubes: Novel platform for multifunctional applications", *Prog. Mater. Sci.*, **69**, 183-212. <https://doi.org/10.1016/j.pmatsci.2014.11.001>.
- Sosa, E.D., Darlington, T.K., Hanos, B.A. and O'Rourke, M.J.E. (2014), "Multifunctional thermally remendable nanocomposites", *J. Compos.*, Article ID 705687, 12. <http://dx.doi.org/10.1155/2014/705687>.
- Wang, C.M., Ma, Y.Q., Zhang, Y.Y. and Ang, K.K. (2006), "Buckling of double-walled carbon nanotubes modeled by solid shell elements", *J. Appl. Phys.*, **99**(11), 114317-114312. <https://doi.org/10.1063/1.2202108>.
- Wang, Q. and Liew, K.M. (2007), "Application of nonlocal continuum mechanics to static analysis of micro-and nano-structures", *Phys. Lett. A*, **363**, 236-242. <https://doi.org/10.1016/j.physleta.2006.10.093>.
- Xu, K.Y., Aifantis, E.C. and Yan, Y.H. (2008), "Vibrations of double walled carbon nanotubes with different boundary conditions between inner and outer tubes", *J. Appl. Mech.*, **75**(2), 021013. <https://doi.org/10.1115/1.2793133>.
- Zhang, Y.Q., Liu, G.R. and Xie, X.Y. (2005), "Free transverse vibrations of double-walled carbon nanotubes using a theory of nonlocal elasticity", *Phys. Rev. B*, **71**(19), 195404. <https://doi.org/10.1103/PhysRevB.71.195404>.
- Zhao, J., Buldum, A., Lu, J.P. and Han, J. (2002), "Gas molecule adsorption in carbon nanotubes and nanotubes bundles", *Nanotechnol.*, **13**(2), 195.
- Zidour, M., Benrahou, K., Semmah, A.W., Naceri, M., Belhadj, H.A., Bakhti, K. and Tounsi, A. (2012), "The thermal effect on vibration of single walled carbon nanotubes using nonlocal Timoshenko beam theory", *J. Comput. Mater. Sci.*, **51**(1), 252-260. <https://doi.org/10.1016/j.commatsci.2011.07.021>.
- Zidour, M., Daouadji, T.H., Benrahou, K.H., Tounsi, A., AddaBedia, E.A. and Hadji, L. (2014), "Buckling analysis of chiral single-walled carbon nanotubes by using the nonlocal Timoshenko beam theory", *Mech. Compos. Mater.*, **50**(1), 95-104. <https://doi.org/10.1007/s11029-014-9396-0>.
- Zidour, M., Daouadji, T.H., Benrahou, K.H., Tounsi, A., Bedia, E.A.A. and Hadji, L. (2014), "Buckling analysis of chiral single-walled carbon nanotubes by using nonlocal Timoshenko beam theory", *Mech. Compos. Mater.*, **50**(1), 95-104. <https://doi.org/10.1007/s11029-014-9396-0>.